BioNanoSci. (2011) 1:97–102
DOI 10.1007/s12668-011-0011-8

Membrane-Mediated Inter-Domain Interactions

Hongyan Yuan · Changjin Huang · Sulin Zhang

Published online: 14 June 2011

Abstract The amazing ability of living cells in achieving strict and robust control of their membrane morphologies and functions over different length scales leads to the concept that membrane domains, such as lipid rafts, are the basic organization units of cellular membranes. Yet fundamental understanding of the membrane-mediated inter-domain interaction still remains incomplete. In the present work, we probe inter-domain interactions by performing coarse-grained molecular dynamics simulations using a highly coarse-grained implicit-solvent fluid membrane model. Our simulations show that the membrane-mediated inter-domain interaction remains repulsive for the contact angle as large as close to 90°. The repulsive interaction force between curved domains increases with the domain curvature and hinders the further domain coalescence. Our findings have broad implications to various biological phenomena such as lipid raft formation, viral budding, and targeted drug delivery.

Keywords Fluid membrane · Membrane-mediated interaction · Spontaneous curvature · Lipid rafts · Domain growth dynamics

1 Introduction

It has been widely accepted that membrane domains of various kinds, such as "lipid rafts" [1] serve as basic units for membrane organization and at the same time as the basic platform for many membrane-mediated functions [2]. While the formation mechanism of lipid rafts in living cells remains a subject of lively debate [3], micrometer-sized lipid domains in model membranes have been directly observed using fluorescent microscopy [4]. Model membranes are usually composed of three types of lipids: unsaturated and saturated lipids, and cholesterols. Below a transition temperature, the ternary membranes are phase-separated into liquid-ordered (consisting of saturated lipids and cholesterol) and liquid-disordered (consisting of unsaturated lipids) phases [5]. It has been well established that the hydrophobic mismatch due to the thickness difference between two phases gives rise to a line tension that drives the phase separation [6].

During the phase separation process in model membranes, anomalous slowing down of domain growth was observed [7], which leads to the speculation that membrane-mediated inter-domain interaction is repulsive. The formation of long-lived regular pattern of circular domains in fluid vesicles widely reported in literature further supports the speculation [4, 8, 9]. Under the small-gradient and zero-temperature assumptions, previous theoretical models have revealed a repulsive interaction between two conical inclusions [10–12]. For example, Weikl et al. [11] obtained the following formula for the interaction energy G between two identical rigid conical inclusions in an infinite large planar membrane with vanishing tension,

$$G(R) = 8\pi B\alpha^2 \frac{r^4}{R^4} + O\left(\frac{1}{R^5}\right), \tag{1}$$

where the center-to-center distance R between the inclusions is assumed to be much larger than the radius r of the inclusions, the contact angle α represents the membrane slope at the boundary of the inclusions under the small-gradient assump-

H. Yuan · C. Huang · S. Zhang (✉)
Department of Engineering Science and Mechanics,
Pennsylvania State University,
University Park, PA 16802, USA
e-mail: suz10@psu.edu

tion (illustrated in Fig. 1), and B is the membrane bending rigidity. The theoretical analysis for the interactions between inclusions may be also applicable to partially budded lipid domains from a mathematical viewpoint [13]. However, the validity of the theoretical prediction with the assumptions such as small-gradient, zero-temperature limit, and $R \gg r$ needs to be justified for physiologically relevant experimental conditions. In addition, contrary to the speculation and theoretical prediction, a recent study predicted attractive interactions between two highly curved domains that are spatially in close vicinity [14]. The overly simplified treatments in theoretical analysis and controversial predictions in literature motivated the present study.

Though lipid rafts in living cells are much more complicated than domains in model membranes, from a physics viewpoint membrane-mediated inter-domain interactions may be considered to be universal, and may play a similar role in the formation of lipid rafts in living cells. In this article, we examine membrane-mediated elastic interactions between curved domains by performing coarse-grained molecular dynamics (CGMD) simulations using our recently developed one-particle-thick fluid membrane model [15, 16]. We start with two-component fluid vesicles phase-separated into flat or curved domains. Such simulations on two-phase fluid vesicles are deliberately conducted to compare with the experimental observations [7]. We next examine and quantify the interactions between two curved domains in a planar membrane by tracking the trajectories of domains.

2 Methodologies

On the length scale much larger than the membrane thickness, fluid bilayer membranes, from the mechanics viewpoint, can be regarded as "thin fluid shells". Their mechanical behaviors are dictated by only a few effective mechanical properties such as bilayer membrane bending rigidity, area compression modulus, in-plane viscosity, line tension between different phases, and spontaneous curvature. In general, there are two approaches to establish a simulation model for fluid membranes at large length scale. In the first class, the numerical scheme is formulated through the space discretization of the continuum theories

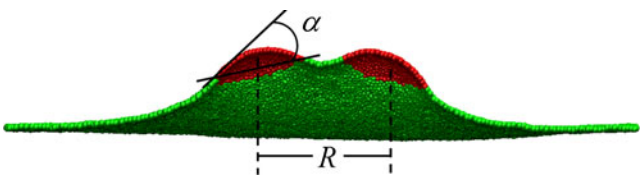

Fig. 1 Side view of a fluid membrane with two curved domains which have contact angle α with the surrounding membrane

of the lipid bilayer membrane. Compared to solid shells [17, 18], the in-plane fluidity and incompressibility conditions of fluid membranes ease analytical formulation of the continuum equilibrium equations [19]. However, the same in-plane fluidity conditions become serious obstacles when numerically implementing continuum theories. As a result, dedicated computational treatments are needed to take into account of the in-plane fluidity and topological changes [20, 21]. The second class is the highly coarse-grained particle-based membrane simulation models [22–25]. Such discrete particle-based models can naturally take into account all the aforementioned dynamical behaviors.

We have recently developed a highly coarse-grained implicit-solvent fluid membrane model [15, 16] for fluid membranes at large length scale. In the model, we simplify the lipid bilayer membrane as a one-particle-thick particle aggregate with out-of-plane bending resistance. The one-particle-thick membrane model neglects the heterogeneity along the membrane thickness direction. Furthermore, an orientation-dependent inter-particle interaction is designed to substitute for the hydrophobic effect that is missing in implicit-solvent membrane models. Such an aggressive level of coarse-graining endows the membrane model high computational efficiency. Besides the inter-particle interaction strength ε, the model introduces three key parameters, μ, ζ, and θ_0, which independently tune, respectively, the bending rigidity, diffusivity, and spontaneous curvature of the simulated membrane. (The readers are referred to Refs. [15, 16] for the detailed mathematical formulations of the model and the physical meanings of the model parameters mentioned above.) The length and time scales of our model are on the order of $\sigma \sim 1.4$ nm and $\tau \sim 0.1$ μs, respectively, which represents the highest level of coarse-graining of this kind. As demonstrated in the applications [15, 16, 26], this membrane model is an accurate and reliable numerical tool to solve the equilibrium or non-equilibrium membrane morphologies or shapes of fluid membranes under various complicated conditions.

To study the dynamics of phase separation, a preassembled vesicle consisting of 11,054 particles is adopted in the CGMD simulations in NVT ensemble (see Ref. [15] for the details of the simulation techniques). The self-assembly of particles into fluid vesicles has been previously demonstrated [15]. We randomly label particles in the vesicle as component A or B with the number ratio A (red): B (green)= 1:2 (see Fig. 2). So component A is the minority particles and clusters of type A particles are considered as domains. The line tension between two phases that drives the phase separation is realized in our simulations by assigning different interaction strength between AA, BB, and AB pairs as: $\varepsilon^{AA}=\varepsilon$, $\varepsilon^{BB}=\varepsilon$, $\varepsilon^{AB}=0.65\varepsilon$. Note that there are several mechanisms [14, 27] by which lipid domains become curved. In model membranes, the domain curvature is a

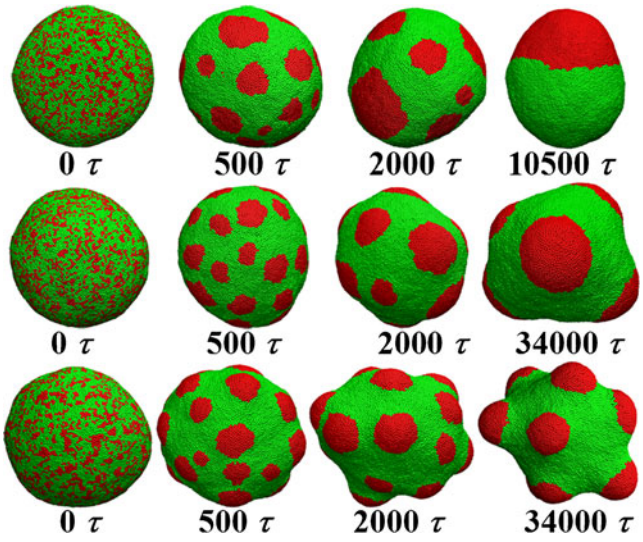

Fig. 2 The domain growth dynamics. Three rows from top to bottom correspond to three different spontaneous curvatures with $\theta_0^{AA} = 0.0°$, $\theta_0^{AA} = 2.3°$, and $\theta_0^{AA} = 4.6°$, respectively

result of the competition between the line tension and the bending energy [13]. A circular domain becomes partially budded when the domain size is on the order of the invagination length B/γ [28], which is defined as the ratio between the bending rigidity B and the line tension γ at the phase boundary. In living cells, the lipid rafts can have an effective spontaneous curvature induced by the transmembrane proteins [29] or scaffolding proteins [30]. The domain size in the following simulations is not large enough to bud the domain. Instead, in the simulations, we induce the domain curvature via the effective spontaneous curvature parameter θ_0^{AA}, which mimics protein-mediated domain formation. For example, assigning $\theta_0^{AA} = 0.0°$ yields flat domain, while assigning $\theta_0^{AA} = 2.3°$ and $\theta_0^{AA} = 4.6°$ leads to curved domains. The spontaneous curvature parameter θ_0 of the formed domain is directly related to the contact angle α. The larger the spontaneous curvature parameter θ_0, the larger the contact angle α, which can be measured from the equilibrium configuration in the simulations using the definition illustrated in Fig. 1. Other parameters used in the simulations are: k_BT=0.20ε, η=2, ζ=4, μ^{AA}=μ^{AB}=6, $\theta_0^{BB} = 0.0$, and μ^{BB}=3, unless otherwise mentioned. The parameter values yield the following membrane properties: vesicle diameter ~60σ, line tension γ~0.35ε/σ, bending rigidity of A component B_A~50k_BT, bending rigidity of B component B_B~25k_BT, the invagination length B_A/γ~29σ, and single-particle diffusion constant D~0.06σ^2/τ.

3 Simulation Results

The domain growth dynamics for three different prescribed spontaneous curvatures of the minority particles is depicted in Fig. 2. Starting with a randomly mixed state, dispersed circular domains quickly form and then undergo a diffusion–coalescence process. The fluid vesicle in the top row with flat domains ("flat" here means having the same spontaneous curvature as the rest of the vesicle) reaches the completely phase-separated state at 10,500τ. The vesicle in the middle row with slightly curved domains has several separated domains even at 34,000τ. Slowing down of domain growth is most evident in the bottom row where the domain curvature is the largest and the domain size is more uniform. These formed domains are strikingly similar to the previous experimental data [7]. As already argued [7, 9, 13], these domains may be kinetically trapped due to the membrane-mediated energy barriers against merging.

Figure 3 quantitatively depicts the domain growth dynamics by plotting the interface length L of the domains as a function of time t. For all the cases, the domain growth dynamics at the early stage (t<2,000τ) follows the same power law $L \sim t^{-\omega}$. From the time-elapsing movies (not shown here) of the simulations, it can be seen that the domain growth follows a diffusion-limiting process. The growth exponent ω of the diffusion-limiting process can be deduced from the relation between the domain diffusion constant D_r and the domain radius r [7]. Assume $D_r \sim r^{-\beta}$ and the diffusion distance between the two nearest domains is proportional to the domain radius, one finds ω=1/(2+β). The growth exponent ω in the early period is fitted as ω=0.32. This value is in close agreement with the diffusion-limiting growth exponent of 1/3 (see the straight line in Fig. 3a) provided D_r~r^{-1}, as well as previous simulations [31–33] and the supported membrane experiments [34]. In the later period, the two curves ($\theta_0^{AA} = 2.3°$ and $\theta_0^{AA} = 4.6°$) deviate from that of $\theta_0^{AA} = 0.0°$ case due to slowing down of domain growth, indicating that domain coarsening during this period is kinetically hindered. The energy barrier against domain merging can be estimated from the delay of domain growth of the curved domains in comparison with that of the flat domains, i.e., $\Delta E = k_BT \ln(t_2/t_1)$, where t_1 and t_2 are the time spent in merging of two domains for the flat and curved domain cases, respectively. For example, by comparing $\theta_0^{AA} = 4.6°$ case with $\theta_0^{AA} = 0.0°$ case, one follows that the largest energy barrier encountered in the case of $\theta_0^{AA} = 4.6°$ is ~2k_BT.

In a bulk fluid, the size-dependent diffusion of spherical particles is well described by the Einstein–Stokes equation, and one finds β=1. In a 2D fluid, the analytical solution of the Stokes equations of a moving cylinder does not exist (the so-called Stokes paradox). By modifying the problems, Saffman and Delbruck [35] obtained equations for diffusion constant of cylindrical objects in 2D fluid and established the logarithmic dependence D_r~ln(1/r). In recent years, reminiscent attention [36, 37] has been focused on the size-dependent diffusion in lipid bilayer membranes because the

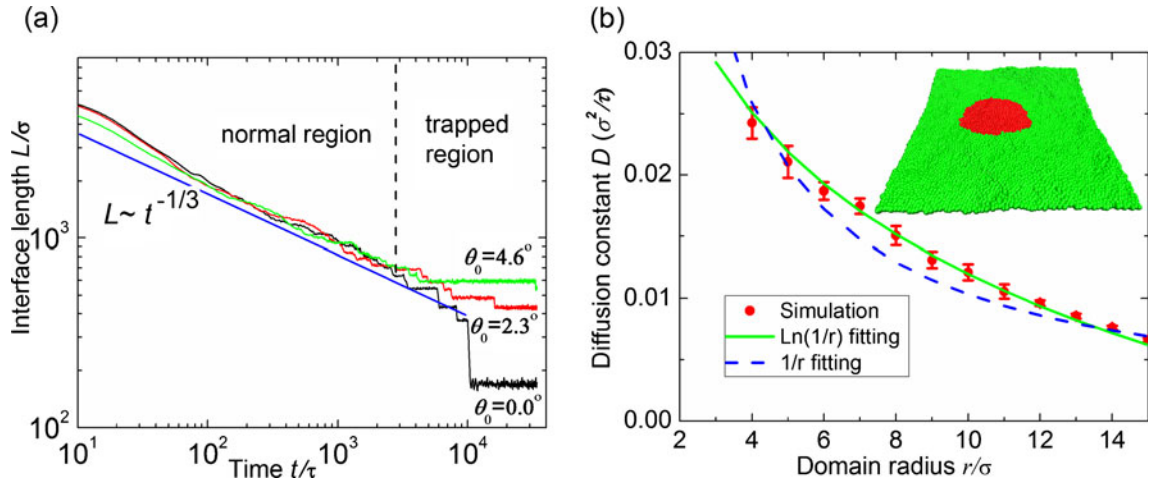

Fig. 3 **a** Interface length as a function of time. Three sets of data correspond to different spontaneous curvatures of component A. The *straight line* is $L \sim t^{-1/3}$. **b** Domain diffusion constant as a function of domain radius

appropriate relation $D_r(r)$ is needed to infer the size of the tracked objects from the measurement of their diffusion constants [38]. We also obtained the domain diffusion constant as a function of domain radius for our membrane model by performing a series of non-equilibrium CGMD simulations. The simulation setup is briefly described as follows. As shown in the inset of Fig. 3b, a sufficiently small "gravity force" is applied to a circular domain along the in-plane direction. The domain is moving at a constant velocity while the driving force is balanced by the friction force from the surrounding particles. The ratio between the settled velocity and the driving force is the mobility b, and the diffusion constant can be obtained by the Einstein equation $D_r=k_BTb$. The domain diffusion constant as a function of domain radius is presented in Fig. 3b, where both $D_r \sim \ln(1/r)$ and $D_r \sim r^{-1}$ fittings are given. Although the logarithmic fitting has better accuracy, the slight deviation of $D_r \sim r^{-1}$ fitting may explain why the growth exponent ω found in Fig. 3 is close to 1/3.

Fluid vesicle simulations presented above are deliberately designed to reproduce the long-lived regular pattern of domains observed in experiments. Next, we attempt to examine the theoretical prediction given in Eq. 1 for the condition under which two curved domains interact in a planar membrane. Note that in order to be mathematically tractable, Eq. 1 was obtained under the assumption $R \gg r$. Here, we study the interaction between two curved domains of radius 12σ with a center-to-center distance 30σ. The energy barrier and interaction force are expected to be quantitatively computed from the simulations. However, as estimated before, the largest energy barrier is about $2k_BT$ in the current simulations due to the small domain size. Thermal fluctuations significantly affect the data extracted from the simulations. Alternatively, since the kinetic time scale is affected by the energy barrier exponentially, the diffusion trajectories of two neighboring domains can be used to infer the nature of the inter-domain interactions, as shown in the following simulations and in Fig. 4. For fluid membranes, out-of-plane undulations (or fluctuations) are excited by the thermal energy and the mean square fluctuation amplitude linearly scales with the absolute temperature and quartically with the undulation wavelength. We found that the simulation results were largely affected by large wavelength fluctuations. In order to obtain decisive results, we damp out the large wavelength out-of-plane fluctuations in the simulations by adding a damping force to the membrane undulations. For the simulations in Fig. 4, two domains are initially held at a fixed distance $R=30\sigma$ until the system is equilibrated. Starting from $t=1{,}000\tau$, the position constraint is released and domains start to

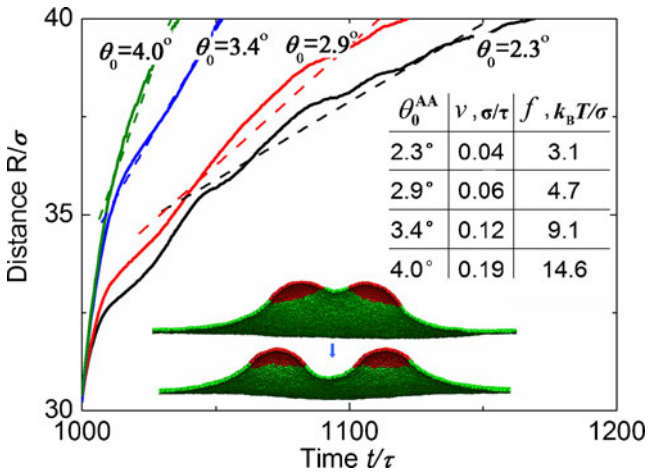

Fig. 4 The distance between two domains in a planar membrane as a function of time. The picture *inset* shows simulation snapshots when two domains diffuse away from each other. The *table* inset shows the average velocities and estimated repulsive forces at different domain spontaneous curvatures θ_0

diffuse. The distance between two domains as a function of time is given in Fig. 4. Four curves in Fig. 4 correspond to four different domain spontaneous curvatures. The contact angle α for θ_0=2.3°, 2.9°, 3.4°, and 4.0° is about 30°, 40°, 60°, and 85°, respectively. The picture inset in Fig. 4 depicts the domain-separating process once the position constraint is released. Continuous separation of two domains occurs in the beginning. Such directed motions are not normal Brownian motions; instead, they are driven by the membrane-mediated repulsive forces.

To extract interaction force from distance–time curves in Fig. 4, we first calibrate the mobility b of curved domains in the absence of elastic interaction force by performing single domain forced motion (same setup as described for Fig. 3b) and b was found to be about $0.065\sigma^2/(\varepsilon\tau)$ for domain radius 12σ. Linear fitting of the distance–time curves yields the average moving velocity v of domains. Note that large fluctuations induced by the background Brownian motions are present in the distance–time curves. For the purpose of estimating the order of magnitude of the interaction force, we simply use a linear fitting for the relatively later region of the curves. The averaged forces for the different domain curvatures can be obtained via the equation $f=v/b$, as shown in the table inset of Fig. 4. We see that the repulsive force increases with the contact angle and remains repulsive even when the contact angle is close to 90° which is far beyond the small contact angle limit.

4 Conclusions

In summary, our CGMD simulations demonstrated that domain growth dynamics depends on the thermodynamic and mechanical properties of the domains. The early stage of domain growth dynamics is a diffusion-limiting process, while the later stage is kinetically hindered. The spontaneous curvature of the minority lipids sets the contact angle of the domains, and the overlapping of the influential zone of the domains results in membrane-mediated inter-domain elastic interactions that give rise to the finite domain size in a relatively long time scale. Our simulations show that the membrane-mediated inter-domain interaction remains repulsive for the contact angle as large as close to 90°. Note that our conclusion is not contradictory to the simulation result in Ref. [14], because the contact angles in their simulations are larger than 90°. The repulsive inter-domain energy explains the formation of the regularly patterned circular domains in model membranes and might attribute to the formation of lipid rafts in living cells.

Acknowledgment We thank financial support from the National Science Foundation under grant no. CMMI-0826841.

References

1. Edidin, M. (2003). The state of lipid rafts: from model membranes to cells. *Annual Review of Biophysics and Biomolecular Structure, 32*, 257–283.
2. Pike, L. J. (2006). Rafts defined: a report on the Keystone Symposium on Lipid Rafts and Cell Function. *Journal of Lipid Research, 47*(7), 1597–1598.
3. Yethiraj, A., & Weisshaar, J. C. (2007). Why are lipid rafts not observed in vivo? *Biophysical Journal, 93*(9), 3113–3119.
4. Baumgart, T., Hess, S. T., & Webb, W. W. (2003). Imaging coexisting fluid domains in biomembrane models coupling curvature and line tension. *Nature, 425*(6960), 821–824.
5. Garcia-Saez, A. J., Chiantia, S., & Schwille, P. (2007). Effect of line tension on the lateral organization of lipid membranes. *Journal of Biological Chemistry, 282*(46), 8.
6. Rietveld, A., & Simons, K. (1998). The differential miscibility of lipids as the basis for the formation of functional membrane rafts. *Biochimica et Biophysica Acta (BBA)-Reviews on Biomembranes, 1376*(3), 467–479.
7. Yanagisawa, M., Imai, M., Masui, T., Komura, S., & Ohta, T. (2007). Growth dynamics of domains in ternary fluid vesicles. *Biophysical Journal, 92*(1), 115–125.
8. Rozovsky, S., Kaizuka, Y., & Groves, J. T. (2004). Formation and spatio-temporal evolution of periodic structures in lipid bilayers. *Journal of the American Chemical Society, 127*(1), 36–37.
9. Semrau, S., Idema, T., Schmidt, T., & Storm, C. (2009). Membrane-mediated interactions measured using membrane domains. *Biophysical Journal, 96*(12), 4906–4915.
10. Goulian, M., Bruinsma, R., & Pincus, P. (1993). Long-range forces in heterogeneous fluid membranes. *Europhysics Letters, 22*(2), 145–150.
11. Weikl, T. R., Kozlov, M. M., & Helfrich, W. (1998). Interaction of conical membrane inclusions: effect of lateral tension. *Physical Review E, 57*(6), 6988–6995.
12. Kim, K. S., Neu, J., & Oster, G. (1998). Curvature-mediated interactions between membrane proteins. *Biophysical Journal, 75*(5), 2274–2291.
13. Ursell, T. S., Klug, W. S., & Phillips, R. (2009). Morphology and interaction between lipid domains. *Proceedings of the National Academy of Sciences of the United States of America, 106*(32), 13301–13306.
14. Reynwar, B. J., Illya, G., Harmandaris, V. A., Muller, M. M., Kremer, K., & Deserno, M. (2007). Aggregation and vesiculation of membrane proteins by curvature-mediated interactions. *Nature, 447*(7143), 461–464.
15. Yuan, H., Huang, C., Li, J., Lykotrafitis, G., & Zhang, S. (2010). One-particle-thick, solvent-free, coarse-grained model for biological and biomimetic fluid membranes. *Physical Review E, 82*(1), 011905.
16. Yuan, H., Huang, C., & Zhang, S. (2010). Dynamic shape transformations of fluid vesicles. *Soft Matter, 6*, 4571–4579.
17. Huang, X., Yuan, H., Hsia, K. J., & Zhang, S. (2010). Coordinated buckling of thick multi-walled carbon nanotubes under uniaxial compression. *Nano Research, 3*(1), 32–42.
18. Huang, X., Yuan, H., Liang, W., & Zhang, S. (2010). Mechanical properties and deformation morphologies of covalently bridged multi-walled carbon nanotubes: multiscale modeling. *Journal of the Mechanics and Physics of Solids, 58*, 1847–1862.
19. Ou-Yang, Z.-C., Liu, J.-X., & Xie, Y.-Z. (1999). In Y.-B. Dai, B.-L. Hao, & Z.-B. Su (Eds.), *Geometric methods in the elastic theory of membranes in liquid crystal phases* (Advanced Series on Theoretical Physical Science). Singapore: World Scientific Publishing Company.

20. Atilgan, E., & Sun, S. X. (2007). Shape transitions in lipid membranes and protein mediated vesicle fusion and fission. *Journal of Chemical Physics, 126*(9), 095102.
21. Feng, F., & Klug, W. S. (2006). Finite element modeling of lipid bilayer membranes. *Journal of Computational Physics, 220*(1), 394–408.
22. Brannigan, G., & Brown, F. L. H. (2004). Solvent-free simulations of fluid membrane bilayers. *Journal of Chemical Physics, 120*(2), 1059–1071.
23. Ballone, P., & Del Popolo, M. G. (2006). Simple models of complex aggregation: vesicle formation by soft repulsive spheres with dipolelike interactions. *Physical Review E, 73*(3), 031404.
24. Kohyama, T. (2009). Simulations of flexible membranes using a coarse-grained particle-based model with spontaneous curvature variables. *Physica A: Statistical Mechanics and Its Applications, 388*(17), 3334–3344.
25. Drouffe, J. M., Maggs, A. C., & Leibler, S. (1991). Computer simulations of self-assembled membranes. *Science, 254*(5036), 1353–1356.
26. Huang, C., Yuan, H., & Zhang, S. (2011). Coupled vesicle morphogenesis and domain organization. *Applied Physics Letters, 98*(4), 043702.
27. Blood, P. D., & Voth, G. A. (2006). Direct observation of Bin/amphiphysin/Rvs (BAR) domain-induced membrane curvature by means of molecular dynamics simulations. *Proceedings of the National Academy of Sciences of the United States of America, 103*(41), 15068–15072.
28. Jülicher, F., & Lipowsky, R. (1996). Shape transformations of vesicles with intramembrane domains. *Physical Review E, 53*(3), 2670.
29. Allen, J. A., Halverson-Tamboli, R. A., & Rasenick, M. M. (2007). Lipid raft microdomains and neurotransmitter signalling. *Nature Reviews Neuroscience, 8*(2), 128–140.
30. Arkhipov, A., Yin, Y., & Schulten, K. (2008). Four-scale description of membrane sculpting by BAR domains. *Biophysical Journal, 95*(6), 2806–2821.
31. Kumar, P. B. S., Gompper, G., & Lipowsky, R. (2001). Budding dynamics of multicomponent membranes. *Physical Review Letters, 86*(17), 3911–3914.
32. Laradji, M., & Sunil Kumar, P. B. (2004). Dynamics of domain growth in self-assembled fluid vesicles. *Physical Review Letters, 93*(19), 198105.
33. Laradji, M., & Kumar, P. B. (2006). Anomalously slow domain growth in fluid membranes with asymmetric transbilayer lipid distribution. *Physical Review E, 73*, 040901.
34. Jensen, M. H., Morris, E. J., & Simonsen, A. C. (2007). Domain shapes, coarsening, and random patterns in ternary membranes. *Langmuir, 23*(15), 8135–8141.
35. Saffman, P. G., & Delbruck, M. (1975). Brownian motion in biological membranes. *Proceedings of the National Academy of Sciences of the United States of America, 72*(8), 3111–3113.
36. Gambin, Y., Lopez-Esparza, R., Reffay, M., Sierecki, E., Gov, N. S., Genest, M., et al. (2006). Lateral mobility of proteins in liquid membranes revisited. *Proceedings of the National Academy of Sciences of the United States of America, 103*(7), 2098–2102.
37. Guigas, G., & Weiss, M. (2006). Size-dependent diffusion of membrane inclusions. *Biophysical Journal, 91*(7), 2393–2398.
38. Pralle, A., Keller, P., Florin, E. L., Simons, K., & Horber, J. K. H. (2000). Sphingolipid-cholesterol rafts diffuse as small entities in the plasma membrane of mammalian cells. *The Journal of Cell Biology, 148*(5), 997–1007.